



Published in final edited form as:

J Magn Reson Imaging. 2020 September ; 52(3): 686–696. doi:10.1002/jmri.26942.

Low-Cost and Portable MRI

Lawrence L. Wald, PhD^{1,2,3,*}, Patrick C. McDaniel, MS^{1,4}, Thomas Witzel, PhD^{1,2}, Jason P. Stockmann, PhD^{1,2}, Clarissa Zimmerman Cooley, PhD^{1,2}

¹Athinoula A Martinos Center for Biomedical Imaging, Department of Radiology, Massachusetts General Hospital, Charlestown, Massachusetts, USA

²Harvard Medical School, Boston, Massachusetts, USA

³Division of Health Sciences and Technology, Harvard – Massachusetts Institute of Technology, Cambridge, Massachusetts, USA

⁴Department of Electrical Engineering and Computer Science, Massachusetts Institute of Technology, Cambridge, Massachusetts, USA

Abstract

Research in MRI technology has traditionally expanded diagnostic benefit by developing acquisition techniques and instrumentation to enable MRI scanners to "see more." This typically focuses on improving MRI's sensitivity and spatiotemporal resolution, or expanding its range of biological contrasts and targets. In complement to the clear benefits achieved in this direction, extending the reach of MRI by reducing its cost, siting, and operational burdens also directly benefits healthcare by increasing the number of patients with access to MRI examinations and tilting its cost–benefit equation to allow more frequent and varied use. The introduction of low-cost, and/or truly portable scanners, could also enable new point-of-care and monitoring applications not feasible for today's scanners in centralized settings. While cost and accessibility have always been considered, we have seen tremendous advances in the speed and spatial-temporal capabilities of general-purpose MRI scanners and quantum leaps in patient comfort (such as magnet length and bore diameter), but only modest success in the reduction of cost and siting constraints. The introduction of specialty scanners (eg, extremity, brain-only, or breast-only scanners) have not been commercially successful enough to tilt the balance away from the prevailing model: a general-purpose scanner in a centralized healthcare location. Portable MRI scanners equivalent to their counterparts in ultrasound or even computed tomography have not emerged and MR monitoring devices exist only in research laboratories. Nonetheless, recent advances in hardware and computational technology as well as burgeoning markets for MRI in the developing world has created a resurgence of interest in the topic of low-cost and accessible MRI. This review examines the technical forces and trade-offs that might facilitate a large step forward in the push to "jail-break" MRI from its centralized location in healthcare and allow it to reach larger patient populations and achieve new uses.

Level of Evidence: 5

Technical Efficacy Stage: 6

*Address reprint requests to: L.W., 149 13th St. Rm. 2301, Charlestown, MA 02129. wald@nmr.mgh.harvard.edu.

WHILE ANY EXPANSION of a healthcare technology must be viewed under the lens of cost-effectiveness analysis,^{1,2} the potential benefits of expanding the accessibility of magnetic resonance imaging (MRI) technology to the world's patient population is clear. The range and depth of geographical MRI accessibility gaps has been recently reviewed by Geethanath and Vaughan, who also review technology development efforts designed to mitigate this problem.³ There are regions of the world that clearly lag worldwide averages in number of scanners or even any scanners at all, although there is some evidence that low-income regions overspend on expensive technology relative to other infrastructure.⁴ The demand problem is not limited to developing countries. Insufficient scanner density in "developed" countries still results in wait-periods prior to diagnostic care.⁵ While accessibility issues are intertwined with other economic, social, and technical problems, they are likely to persist as until the relative cost of MRI is reduced relative to other healthcare technologies.

Because the data compiled by Geethanath and Vaughan clearly spell out the depth of the worldwide accessibility variance,³ our review focuses on assessing progress and prospects for cost reduction. Although many factors play a role in MRI examination costs, or even the marginal cost of adding a scanner, we focus mainly on the equipment costs and the major infrastructure and maintenance cost repercussions of the equipment. Ongoing steady but gradual cost reductions of today's designs will result from the commoditization of components, but we focus instead on the potential for radical changes in cost and portability. We partition the MRI scanner into its component groups: 1) the magnet together with siting considerations, cryogenic systems, and power supplies (if required); 2) the image encoding unit (ie, the gradient coil and drivers in a traditional scanner); 3) the RF subsystem including transmit amplifier and coil and receive coils; and 4) the console (small signal components) and computational system.

We do not provide a detailed accounting of component costs, as this requires detailed specifications, but attempt a general overview with a focus on areas of technological innovations/barriers and trends that might significantly reduce cost. We focus on the cost per scanner, not the cost per scan, thus omitting some important strategies to reduce diagnostic costs such as increasing patient throughput by increased imaging speed and workflow advances. Such innovations might allow a high-cost scanner to economically outperform a low-cost unit. Finally, we try to separate evolutionary trends by which the canonical scanner architecture is simply refined from more radical design changes. The latter will likely impose limitations on how the images are acquired, for example, limiting the type of images, spatial resolution, and signal-to-noise ratio (SNR). These are important trade-offs that can only be superficially evaluated in this review. Commonly discussed strategies such as reduction of the B_0 field below that of the market dominating high-field systems (1.5T and 3T) fall into this category, as do systems employing inhomogeneous or prepolarized B_0 field systems. The trade-offs imposed by these steps constitute a major change in the way MRI is acquired, but are likely needed to significantly expand MRI's use into portable or point-of-care (POC) applications, or for moving from diagnostics to monitoring. Some approaches, such as low-field MRI have been recently reviewed.⁶

Lessons From Other Modalities

Transition from hospital-centric to portable diagnostic devices is nearly as old as radiology itself. The x-ray was discovered in late 1895 and was used clinically within a year. It became a mobile imaging technology in 1914 when Marie Curie pushed to develop a fleet of x-ray-equipped ambulances for use in World War I to assist surgeons in field hospitals (see Fig. 1). By comparison, 45 years after MRI's introduction we still lack a truly portable MRI. Here we define "portable" as a device that can be moved room-to-room by a single nurse for use on an individual patient within minutes of arriving. In the truly portable scanner case, the power and cooling infrastructure of a typical office or exam room must be sufficient. This contrasts with currently existing "mobile" MRI scanners inside truck trailers that require a road, dedicated power, and cooling infrastructure waiting at the new site, and a minimum of tens of hours of setup prior to imaging at the new location. Note, there are also solutions between conventional and true portable/POC solutions where some special infrastructure is provided in the room.

In this article we make the case that the challenges of achieving portable and low-cost MRI are rooted in the insensitivity of MRI, which is typically addressed by using high-field, highly homogeneous magnets. The associated bulk and complexity of such magnets, together with their associated cryogenic subsystems, creates barriers to lowering cost and operation as a portable or POC device. Additionally, issues arise from the safety aspects of the fringe fields and the large gradient current and heat dissipation and the need to fit within conventional "office" space, power, and cooling infrastructure. To achieve all this, the contemporary use-model where one scanner is expected to address all possible MRI examinations might need to be reexamined. Thus, the goal becomes low-cost portable scanners that can achieve a useful range of clinical services, but perhaps not all. Before exploring the detailed prospects for dramatically lowering cost and/or creating a portable or POC MRI, it is valuable to examine other modalities that have already traversed this path. Although the case-study of portable and POC ultrasound (US) and computed tomography (CT) is informative, it is an open research question how to achieve the same goal with MRI.

Portable US

US is the obvious example of a fully portable and POC diagnostic imaging modality. It is now readily commercially available in a range of sizes and capabilities, ranging from trolley/cart-sized devices found in centralized radiology facilities, to laptop sized "compact" units, to hand-held POC scanners.⁷ Compact US units comprised 29% of the units shipped in the \$6.6 billion USD ultrasound market of 2017, while handheld devices comprised 3%. Nonetheless, handheld devices were the segment with the largest growth (IHSMARKIT analysis).⁸ The MRI market is smaller and, no doubt, not a direct analogy, but the success of the multiple US scanner sizes and portability ranges delivers several messages. The MR community can learn several lessons from US. First, all scanners are not required to be equal in their capabilities; the market is capable of deciding when to use which scanner; effectively trading-off imaging capability for portability and cost. Second, it is likely that the range of devices significantly extends the reach of diagnostic US.⁷ Finally, a significant equipment

price drop (>10×) and extreme portability seems to be driving the successes of portable US. It remains to be seen if MR can match these achievements

Portable CT

Portable CT scanners, although not as small or ubiquitous as their US counterparts, are readily commercially available.⁹ They bring CT scanning to interventional and interoperative suites,^{10,11} intensive care units,^{12,13} emergency departments,¹⁴ and ambulances.^{15,16} Although they have shielding challenges, they can operate with standard power and cooling infrastructure. However, the use of CT, especially in pediatrics, may carry risks. In a 15-year retrospective study of pediatric CT scans, Miglioretti et al estimate that the ~4 million pediatric CT scans will cause 4870 additional cancers in the U.S., although simple dose reduction might significantly decrease this.^{17,18} The success of portable CT, together with the complementary diagnostic value possible from MRI, suggests an MRI scanner with similar portability could find a role in these settings now uniquely occupied by CT scanners.

Desktop and Single-Sided NMR Spectrometers

Although not a medical diagnostic tool, the recent advent of "desktop" nuclear magnetic resonance (NMR) spectrometers¹⁹⁻²² merits discussion as a technological close-cousin of MRI. For many years, the NMR spectrometer market was nearly exclusively the domain of superconducting solenoid-based magnet systems, usually operated in a central NMR core service facility. Thus, the NMR spectrometer world of 10 years ago was analogous to the clinical MRI world today. However, recent advances in permanent magnet design,²³⁻²⁵ and the sophistication of a field programmable gate array (FPGA) and similar electronics has allowed the deployment of low-cost, easy to site, bench-top systems with footprints of less than 1 m².²⁶ These systems do not provide the spectral resolution or sensitivity offered by ultrahigh-field superconducting magnet systems, but allow the chemist to analyze a range of samples at the bench, without the trouble and expense of using the considerably costlier high-end systems. They also allow NMR to be more easily incorporated as a monitoring device in the chemical reaction process. Bench-top spectrometers have been applied to food analysis,²⁷ interoperative flow,²² and exist as "single-sided" devices, allowing NMR spectra to be recorded for samples outside the magnet.^{21,28}

The creation of successful MR depth-profilers that measure a 1D image of samples external to the magnet constitutes a second recent technology with potential to extend the reach and accessibility of MR. Single-sided depth profilers such as the NMR-Mouse use a built-in field gradient outside the magnet to provide a 1D depth profile from the Fourier transform of the recorded MR signal.²⁹ MR depth profilers have been used to analyze artwork,³⁰ burn depth,^{31,32} skin layering,³³⁻³⁵ and extended to 2D³⁶ and 3D imaging.³⁷ Similar devices operate in the oil-well logging industry, where outward-looking NMR spectrometers lowered into the borehole record T₂ and diffusion information that informs operators of the properties of the porous rock in the well.³⁸ Recent work has demonstrated 1D, 2D, and 3D imaging over a limited region in a brain-sized instrument,³⁹ and a commercial low-field single-sided prostate imager is under development for use in urology clinics.⁴⁰

Cost of an MRI Scanner

Before reviewing the prospects for lowering the costs of the subsystems found in MRI scanners, or assessing alternative MRI acquisition strategies, it is worth reviewing the goal set by conventional 1.5T scanners. A simple-sounding concept such as "cost" is surprisingly multifaceted.⁴¹ We consider primarily the potential purchase price of the scanner itself, knowing full-well that considerable additional cost factors are at play. For this purpose, we consider the low-end, but highly functional end of the 1.5T superconductor based MRI segment as well as low field (0.2T to 0.35T) clinical vertical-field "open" systems. It is important to note that as the initial purchase price of these systems is reduced, siting, infrastructure, and operating costs are also relevant.

Unfortunately, most market information is proprietary. A 2011 report by the UK National Health Service reported that they paid an average of \$1.4M USD (in the exchange rate at the time) to purchase and site each of the 267 new MRI scanners it installed in the previous 10 years (predominantly 1.5T scanners).⁴² A 2010 study of 28 Belgian hospitals found that the average initial cost for five new 1.5T scanners installed in 2006–2008 was \$1.5M USD (in the exchange rate at the time).⁴³ New "low-end" (but fully functional and general purpose) 1.5T scanners can reportedly be currently purchased for between \$600,000 and \$800,000 USD.⁴⁴ Therefore, a likely cost target for a quantum leap in affordability is likely a factor of 2× below this; more if the scanner has reduced applicability or performance. Many MR researchers think of equipment costs in terms of a "parts-cost." For medical equipment, this is typically 4× to 5× lower than the purchase price. Therefore, we are looking for a solution with a hardware parts cost of below \$75,000 USD. Siting costs become a significant factor, with RF-shielded rooms costing as much as \$100,000 USD. Additional siting costs stem from installing helium quench vents, large electrical feeds, and cooling water.

The "parts costs" of the individual components of the MR system (such as magnet, RF amplifier, etc) are considered proprietary information by manufacturers and are not readily available. While it is possible for individual researchers to purchase these items, what is available is generally more general-purpose laboratory-grade versions from companies catering to that market and not mass-produced components used by the clinical companies. For example, we can have some idea what a magnet company would charge for a single laboratory use 1.5T magnet, but the incremental cost of a magnet in a batch of 1000 is presumably much cheaper. Despite the difficulty of obtaining data on these proprietary component costs, which also depends, of course, on exact specifications, Fig. 2 estimates the relative component group costs for a low-end 1.5T superconducting magnet scanner.

The total cost of ownership for the MR system includes many additional factors beyond the equipment costs. Many of these likely have strong regional variation (such as building renovation and service/maintenance costs) and are not considered here. We include discussion of such factors only to the extent that they can be impacted by system design choices, such as the potential to eliminate RF shielding, cryogen quench vents, cooling infrastructure, or specialized electrical feeds.

Magnets

Superconducting Magnets

Persistent mode superconducting solenoid designs and variants comprise the vast majority of MRI magnet systems. Benefits include stability, homogeneity, and potential for high magnetic field generation.⁴⁵ Wire costs dominate the magnet construction costs and liquid helium (LHe) and refrigeration system (cold-head) maintenance dominate magnet operating costs. Siting and portability is compromised by the size and weight of the magnet (typically on the order of 3000–6000 kg for a 1.5T actively shielded whole-body magnet),⁴⁶ a relatively large magnetic footprint even for actively shielded solenoid designs, the fragile nature of the cryogenic system, and the infrastructure for the LHe quench vent.

The magnet cost is largely a function of wire type and length. For a given field strength, wire length is dictated by a design trade-off between the diameter of the homogeneous spherical volume (DSV), the magnet bore diameter (D), and the magnet length (L). The conductor placement is typically optimized to achieve a minimum cost design with an acceptable trade-off between these three parameters (DSV, D, and L). Xu et al looked at 100 constrained designs for a DSV with 1 ppm homogeneity.⁴⁷ They show that for a given homogeneity ppm specification (eg, 1 ppm), the problem can be cast using only two independent variables (D/DSV) and (L/DSV). Optimizing magnet cost (wire length) formed classic "l-curve" trade-offs between cost and the two variables (D/DSV) and (L/DSV). Selecting the "knee" of the l-curve as the design point for L_{opt} , they found a simple relationship for cylindrical magnets: $L_{opt} = 1.18 \text{ DSV} + 0.77 \text{ D}$, and show that modern designs adhere to this law. While magnets with the desired homogeneity specifications can be designed with shorter lengths ($<L_{opt}$) the wire cost rises exponentially (see Fig. 3). They conclude that the best way to decrease cost is to decrease bore size. This, in turn, puts pressure on the gradient and RF engineers to cede territory.

Of course, lowering field strength will lower magnet cost, as does relaxing homogeneity constraints. Both of these will be examined below. Other ways to reduce cost with conventional solenoid designs include finding an affordable wire alternative with higher current density or reducing cryogenic costs. New types of superconducting wires do not appear often and copper-sheathed NbTi remains the mainstay, but its 9.3K critical temperature requires 4K operation. In contrast, MgB_2 , ReBCO, YBCO, and BSCCO are potential entrants with higher critical temperatures,⁴⁸ although the price per kAm increases dramatically. The wire cost of these high-temperature superconductors is such that it is currently more economical to operate them at low temperature where their critical current is higher, thus reducing wire length.

In cryogenics, the recent decade has brought revolutionary advances in cryogenic cooling systems. Modern cold-heads can now operate at temperatures of 4K with sufficient heat removal to allow modern clinical magnets to operate with "zero boil-off." Thus, although they contain 500 or more liters of LHe, the cryocooler effectively recondenses the evaporating liquid, eliminating the need to replenish LHe under normal operation. This is fortuitous, since the world's helium supply, while apparently sufficient in principal, is

dominated by a small number of suppliers and has proven highly volatile, with escalating costs⁴⁹; a situation that is unlikely to improve in the future.

The next step is a "nearly-dry" magnet using a sufficiently small LHe volume to safely eliminate the quench vent system. The final step is the so-called "dry" or "conduction cooled" magnet; a magnet containing no LHe. Multiple commercial small-bore dry magnets are available, and at least one nearly-dry clinical system. Modern MRI cryocoolers (possibly with two per magnet) can achieve the heat removal needed for a dry or nearly-dry operation, utilizing either the Gifford-McMahon (GM) cycle or a pulse-tube system⁵⁰ to remove a watt of heat at 4K. The truly dry mode is appealing since cryogenics are not even needed at installation, and the LHe vessel can be omitted from the cryostat. But dry operation requires a direct heat path (mechanical connection) between the cryocooler cold stage and the magnet thimble (thus the term "conduction cooling"). In this case, special care must be taken to avoid mechanical vibrations from the cryocooler from being directly transmitted to the magnet, which could induce field instabilities. Additionally, dry magnets are dependent on continuous operation of the cryocooler. The magnet will quickly warm above the critical temperature of the superconducting wire if the cryocooler stops operating. This increases system vulnerability to power or cooling water loss. The ride-thru time can be extended by increasing the cold-mass; however, this would also result in longer startup/quench recovery times.

Modern GM cryocoolers are cheaper pulse-tube cryocoolers, but produce mechanical vibrations associated with the well-known "washing-machine" sound heard in every clinical scanner. In a traditional cryostat with LHe bath, the cryocooler is mechanically uncoupled from the magnet cold-mass; the cryocooler is connected only to the cryostat's radiation shields and a second stage to a recondenser plate which reliquefies the rising gas in a zero boil-off design. GM cryocoolers also require maintenance every ~2 years, a significant operating cost. Pulse-tube cryocooler designs can be made without moving parts in the low-temperature subsection, offering mechanical stability and an improved maintenance life-cycle. There is a nearby moving piston, however, and unfortunately it usually contains a relatively strong paramagnet, potentially disrupting the B_0 field. These problems notwithstanding, it seems likely that conduction cooled clinical MRI magnets will become available.

Reducing the diameter of superconducting magnets and focusing on a specific body part reduces magnet cost size and weight and has been applied to head, extremity, and neonatal scanners at conventional field strengths (1.5T and 3T). For example, the GE neonatal 1.5T scanner has a 52-cm bore length and weighs 408 kg.⁵¹ A recent commercial effort has coupled these strategies in a small solenoid head-only, conduction-cooled 1100 kg magnet at 0.5T.⁵² Another effort, funded by the NIH Brain Initiative, utilizes a 1.5T asymmetric "hair-dryer" style design with relaxed homogeneity specifications and high-temperature superconductors.⁵³

Adjusting the standard superconducting solenoid design to permit true portability would pose several challenges if it was intended to be wheeled around while at field. Solenoid designs have large fringe fields, which would complicate movement logistics, and the

design would have to be highly shielded or readily ramp-able. Extensive shielding with superconducting windings leads to reduced efficiency, increased wire costs, and larger size (the shielding windings are typically large diameter). Shielding with an iron yoke adds considerable weight. Movable superconducting high-field magnets have been achieved over a limited movement range (such as the IMRIS interoperative system), but quench ventilation and cryogenic stability are challenging. Because of these issues, true portability will likely require a low-field or very low-field device where resistive magnets or permanent magnets lacking the cryogenic concerns become feasible.

Low-Field Permanent Magnets

Although low-field superconducting magnets are an option for reducing cost and footprint, once the field is lowered into the $<0.3\text{T}$ range, the cryogenic system will likely dominate cost and other cheaper, simpler options are typically turned to including resistive magnets and permanent magnets. Resistive magnets incur heat dissipation challenges and add the cost of a stabilized power supply. Permanent magnet designs benefit from the stored energy in the magnetized material and power-free and cryogen-free operation, although they require some form of temperature control to stabilize the B_0 field.

Strong permanent "rare-earth" magnets have been available since the early 1980s when the first sintered NdFeB rare-earth magnets were introduced.⁵⁴ Early clinical low-field systems used a permanent magnet dipole design with iron yoke flux return such as the GE Signa Profile (0.2T), the Siemens Magnetom C! (0.35T), and the Hitachi AIRIS (0.3T).⁵⁵ Although known for being "open," the iron yokes and the rare-earth material itself made these systems heavier than 1.5T superconducting solenoid magnets. Nonetheless, with specialized applications and homogeneity relaxation, the magnet weight can be reduced to the portable level. For example, a 200 kg, 0.2T dipole permanent magnet with iron yoke has been recently operated in a minivan for imaging elbow injuries in baseball.⁵⁶

Since these initial dipole-based low-field permanent MRI systems, a series of array-based designs have appeared following the work of Halbach.²⁴ Assembling the magnetized blocks into arrays leads to a wealth of interesting configurations, many of which have recently been reviewed.⁵⁷ The Halbach cylinder is an attractive choice for MRI. RF engineers will recognize it as being the permanent magnet analog of a birdcage RF coil. Phasing the magnetization direction angle from 0 to 4π creates a uniform field transverse to the cylinder axis.

For an idealized Halbach cylinder, the B_0 strength is simply related to the remnant magnetization (B_r) of the material and the inner (r_i) and outer (r_o) radius of the cylinder: $B_0 = B_r \ln(r_o/r_i)$. Thus, $B_0 = 0.51\text{ T}$ for a head sized magnet with $r_o = 36\text{ cm}$ and $r_i = 25\text{ cm}$ using N50-grade NdFeB ($B_r = 1.4\text{ T}$). In practice, the fields are lower due to gaps between the discretized magnet segments and the finite cylinder length. An idealized Halbach cylinder also has no flux density outside the cylinder, suggesting that these are very self-shielded designs. Figure 4 shows flavors of the Halbach cylinder. Useful variants include oppositely oriented NdFeB and SmCo Halbach units in a configuration that cancels the temperature coefficient.²³

Some form of permanent magnet array has formed the basis of several current small-bore (preclinical) systems designed for cost and easy siting, including the Aspect Imaging M3 and M7 and the Bruker Biospin Icon 1T scanner. Aspect Imaging also makes a 510k cleared neonatal scanner (Embrace) and wrist scanner (Wristview). Although the cost of rare-earth materials is volatile, the materials cost of a head-sized magnet is relatively cheap (under \$10,000 USD) and can weigh as little as 120 kg.⁵⁸ Several Halbach cylinders have been constructed with the goal of a low-cost brain MRI⁵⁸⁻⁶⁰ including with the use of magnet motion for image encoding.⁵⁸⁻⁶⁴ Figure 5 shows a prototype 80 mT brain scanner based on an optimized Halbach array⁵⁸ with built in gradient for rotational projection encoding.⁵⁹

Ultra-Low Field (ULF) Magnets

Further reduction of the B_0 field below the ~20 mT lower limit of "low field MRI" results in further savings in magnet costs. Here, resistive electromagnets and very large field of view or very light-weight permanent magnet configurations are possible.^{65,66} But challenges arise from limited SNR. The work on ULF systems has been elegantly reviewed by Kraus et al.⁶⁷ The SNR issues have been addressed by prepolarization methods,^{66,68,69} SQUID, or atomic magnetometer detection,⁷⁰⁻⁷² the use of hyperpolarized media,^{73,74} or very efficient pulse sequences such as balanced steady-state free precession (bSSFP).⁷⁵ In some cases the "fix" to the SNR problem might be more costly than a higher strength magnet. Beyond the SNR problem, challenges arise from concomitant gradient fields and the bandwidth of RF coils (even modest Q tuned circuits have a narrower bandwidth than desirable).

Image Encoding (Gradient) System

Image encoding typically employs a 3-axis gradient system. However, modern parallel imaging acquisitions omit a substantial fraction of gradient encoding steps in k -space and make up for this with geometric information from the RF receive coil array.^{76,77} This trade-off between the gradient and receive subsystems potentially affords system designers the ability to choose where to place their resources. The low-power electronics in the receive system may better commoditize, allowing cost reduction from reduced gradient coil performance with accompanying reductions in electrical power and cooling infrastructure.

If the clinical use cases can be restricted, tailoring the gradient design to specific clinical applications (such as extremity or brain) is an attractive direction for reducing the size, cost, and power needs. In applications where the size of the coil can be reduced, the stored energy in the magnetic field is greatly lowered, since this scales as the volume of the gradient coil. The smaller coil delivers considerably more efficiency (field gradient per ampere of current). Thus, a knee or even head-only gradient is multifold more efficient than a whole-body system, lowering gradient driver costs, conductor cost, and cooling subsystem complexity.

A second level of cost reduction could potentially come from building in a "permanent" gradient into the magnet and utilizing that field for either readout or slice select. The MagneVu (Carlsbad, CA) wrist MRI used a 0.2T U-shaped magnet weighing about 90 kg with a static gradient in the B_0 operating as a slice select gradient.⁷⁸⁻⁸⁰ Recent work has used the built-in gradient of a head-sized Halbach magnet for readout encoding of a RARE spin-echo train sequence, including rotating the magnet to acquire the additional radial

projections needed for a 2D image.⁵⁹ The use of the built-in gradient for a readout requires a spin-echo to refocus the magnetization but it eliminates the need for a switched gradient coil in this direction. Note that the readout gradient has a special role in MRI in that it must dominate the other gradients present, for example, from an inhomogeneous magnet. Phase encode gradient blips surrounding the 180 refocusing pulses in a spin-echo sequence do not have this requirement, since the spin-echo mechanism refocuses the magnet inhomogeneity. In this way, phase encoding works even in very inhomogeneous fields.³⁶

Thus, for a system whose magnet cost has been reduced by relaxing homogeneity constraints, the use of a built-in gradient and spin-echo-based sequence is attractive because it eliminates one of the three gradient coils and amplifier channels. A second gradient channel can be eliminated by rotating the magnet a small amount (1–3°) per repetition time (TR) period to achieve radial in-plane encoding.⁵⁹ Silent or near-silent operation is a side benefit of eliminating the large switching readout gradient. Most of the desired MR contrasts are readily available with spin-echo or RARE-type techniques, including proton density, T₂, FLAIR prepped T₂, and T₁ (with an inversion prep). Even diffusion weighting can be seen. This is common in the well-logging industry where diffusion weighting from the effects of diffusion in the permanent field gradient is uncovered by modulating the RARE echo-train timing.³⁸ However, gradient echo sequences such as the T₂*-weighted images are not possible with a static readout, but little T₂* contrast is possible at low field anyway.

Finally, although shielded gradients were an enabling technology to today's high-field MRI scanners, significant efficiency improvements and accompanying cost reduction could be achieved by eliminating the shielding windings. The shielding windings greatly reduced the eddy currents generated on the magnet bore and cold conducting structures within the cryostat and magnet. As such, cryogenic-free designs are perhaps more amenable to this, since they lack the cold, conducting structures. Other approaches might also impact this problem, including improved preemphasis, dynamic field monitoring systems⁸¹ coupled with incorporation into image reconstruction.⁸²

RF Subsystem, Console, and Computational System

To a first approximation, the RF transmit and receive needs of portable and low-cost MRI are identical to conventional systems at that field strength, since high sensitivity and some degree of parallel imaging are likely still needed. We note that POC use by less expert users would suggest an emphasis on simplicity, and a specialized scanner (for a particular set of clinical applications) might not require the breadth of coils found in a standard clinical MRI suite. The RF subsystem adds cost mainly through the high power RF amplifier system needed for spin excitation. Typically, >20 kW of peak power is needed, but this scales with the excitation coil volume and can thus be greatly reduced for dedicated scanners. For example, only about 5 kW is needed for a head scanner and less for an extremity scanner. Reducing the B₀ field also increases the power efficiency of excitation, since tissue losses dominate the power dissipation (above ~0.5T) and scale as the square of the frequency. Low-cost RF power amplifiers have been introduced to try to support accessible MRI efforts, including an ~3000 €1 kW open-source effort.⁸³ Other approaches include efficient

switched mode modular RF amplifiers with the potential to be placed directly on the RF transmit coil.⁸⁴⁻⁸⁶

The RF receive system costs can escalate with a large number of parallel channels. To this end, commoditization of these small-signal units could further reduce cost. Full-scale integration efforts are underway to reduce an MRI preamplifier and receiver (including ADC) into a single CMOS chip for mounting on each receive coil element.^{87,88} These single-chip MR receiver systems might aid the development of hand-held (single-sided) MR devices, as well as their original goal of creating wireless receive coils.

Conventional MRI consoles retain their high cost despite continued advances and cost reductions in the electronics behind them. The high cost results from nonrecurring development costs and low-volume production of specialized hardware components in the console, as suitable off-the-shelf components are not available for many parts of the MRI console. Although several inexpensive (\$2,000 to \$10,000) MRI consoles have been developed with other approaches,⁸⁹⁻⁹¹ many of the MRI specialized RF signal chain components and signal processing modules can be implemented with a modern FPGA. Implementing fully digital transmitters and receivers in FPGA hardware means that less specialized analog electronics are needed. The console then essentially becomes a software project with substantially lower hardware development costs. For example, an open-source FPGA MRI console based on the \$349 USD STEMLab/Red Pitaya device has recently been described for controlling and acquiring spin-echo, gradient echo, single shot echo-planar imaging, and single-shot spiral imaging.^{92,93} This system uses Xilinx Zynq 7010 SoC, two 125 Msps 14-bit resolution ADCs, and two 125 Msps 14-bit resolution DACs and 16 DIO pins connected to the programmable logic. The entire pulse sequence execution and real-time control are performed by the integrated Dual-Core ARM9 CPUs running at a clock speed of 866 MHz and running software on an embedded Linux OS. The result is two fully programmable transmit and two receive channels that directly synthesize and digitize between signals between DC and 40 MHz (suitable for low-field systems). The \$349 price tag underscores how the console of a low-cost system could be dominated entirely by software development costs.

Another aspect of console cost for conventional clinical systems is the rather large software applications environment and the cost of development and maintenance of this software. This perhaps exceeds the cost of the hardware. Low-field portable MRI systems are often designed for specific purposes, and therefore should be able to operate with a much smaller focused software environment, rather than providing all the applications a general-purpose clinical MRI device demands. Additionally, open-source sequence and image reconstruction projects are underway⁹⁴ and can potentially reduce software development costs. Finally, we note that some of the strategies proposed for low-cost systems will require model-based iterative image reconstruction methods.⁹⁵ This will likely entail retaining a full-power image-processing computer or moving the image reconstruction to a cloud-based system.

Other Components

Other components, such as the patient table, depend more on driving the cost out of manufacturing. RF coils tend to have a high cost relative to component costs, which likely reflects development costs.

Potential Clinical Applications of Low-Cost, Portable, and POC MRI

Broad and impactful applications are needed to drive the considerable technical effort required to significantly reduce cost or create truly portable or POC MRI. The potential directions are likely different for each of these three cases. Low-cost MRI could be immediately useful in providing access to all the many existing clinical applications of MRI for those patients for whom insufficient scanner resources exist.³ A lower cost and the improved footprint associated with portability also allows MRIs to be sited in facilities normally lacking MRI scanners, such as Emergency Departments, ICUs, and recovery rooms, as well as smaller health clinics. A sufficiently inexpensive scanner does not need to be as heavily utilized to recoup investment. Note that a low-cost device can add value even if it cannot perform all possible MRI examinations.

Clinical applications for portable and POC devices are harder to foresee. Since truly portable or POC MRI scanners are not yet commercially available, we can only speculate that they could take over some of the applications currently served by portable CT, where MRI can offer better soft-tissue contrast or repeated x-ray doses are undesirable. The safety of a repeated application of MRI suggests that POC MRI devices might find applications more resembling patient monitoring than a traditional diagnostic role. The difficulty of intracranial monitoring with other modalities suggests a possible role for POC MRI.

Conclusion

A series of technical design advances and system topology innovations are significantly shifting the landscape of what the MRI of the future can look like. Based on the successes other medical imaging modalities have gained by increasing accessibility and addressing POC markets, any morphology changes that MRI scanners can undertake are likely to pay off by extending benefits to existing patients and reaching new populations of patients. Although no truly portable commercial MRI scanner has been introduced to date, considerable work has been put into the feasibility of such a system, including light-weight, low-field extremity and brain magnets with the needed mobility. Further work in this direction is poised to provide insight into the clinical utility of such systems.

Acknowledgment

Contract grant sponsor: National Institute of Biomedical Imaging and Bioengineering of the National Institutes of Health; Contract grant number: R01EB018976.

The authors thank Matthew Rosen for many useful conversations about low field, ultra-low field, and low-cost MRI.

References

1. Hutubessy R, Chisholm D, Edejer TT. Generalized cost-effectiveness analysis for national-level priority-setting in the health sector. *Cost Eff Resour Alloc* 2003;1:8. [PubMed: 14687420]
2. Singer ME, Applegate KE. Cost-effectiveness analysis in radiology. *Radiology* 2001;219:611–620. [PubMed: 11376244]
3. Geethanath S, Vaughan JT Jr. Accessible magnetic resonance imaging: A review. *J Magn Reson Imaging* 2019. Epub 2019/01/15. doi: 10.1002/jmri.26638.
4. Lazaro P, Beerra A, Luengo S, Moteagudo JL, editors. Health care expenditures and expensive medical technology; the paradox of low-income countries. In: *Annual Meeting Int Soc Technol Assess Health Care*; 1994. p 31.
5. Emery DJ, Forster AJ, Shojania KG, Magnan S, Tubman M, Feasby TE. Management of MRI wait lists in Canada. *Healthc Policy* 2009;4:76–86. [PubMed: 19377359]
6. Marques JP, Simonis FFJ, Webb AG. Low-field MRI: An MR physics perspective. *J Magn Reson Imaging* 2019;49:1528–1542. [PubMed: 30637943]
7. Moore CL, Copel JA. Point-of-care ultrasonography. *N Engl J Med* 2011;364:749–757. [PubMed: 21345104]
8. The global ultrasound equipment market in 2018: IHS Markit; 2018. Available from: <https://cdn.ihs.com>.
9. Rumboldt Z, Huda W, All JW. Review of portable CT with assessment of a dedicated head CT scanner. *AJNR Am J Neuroradiol* 2009;30:1630–1636. [PubMed: 19661166]
10. Wallace MJ, Kuo MD, Glaiberman C, Binkert CA, Orth RC, Soulez G, Technology Assessment Committee of the Society of Interventional R. Three-dimensional C-arm cone-beam CT: Applications in the interventional suite. *J Vasc Interv Radiol* 2008;19:799–813. [PubMed: 18503893]
11. Gupta R, Cheung AC, Bartling SH, et al. Flat-panel volume CT: Fundamental principles, technology, and applications. *Radiographics* 2008;28:2009–2022. [PubMed: 19001655]
12. Peace K, Wilensky EM, Frangos S, et al. The use of a portable head CT scanner in the intensive care unit. *J Neurosci Nurs* 2010;42:109–116. [PubMed: 20422797]
13. Butler WE, Piaggio CM, Constantinou C, et al. A mobile computed tomographic scanner with intraoperative and intensive care unit applications. *Neurosurgery* 1998;42:1304–1310; discussion 1310–1311. [PubMed: 9632189]
14. Novelline RA, Rhea JT, Rao PM, Stuk JL. Helical CT in emergency radiology. *Radiology* 1999;213:321–339. [PubMed: 10551209]
15. Ebinger M, Winter B, Wendt M, et al. Effect of the use of ambulance-based thrombolysis on time to thrombolysis in acute ischemic stroke: A randomized clinical trial. *JAMA* 2014;311:1622–1631. [PubMed: 24756512]
16. Ebinger M, Grittner U, Audebert HJ. Ambulance-based thrombolysis in acute ischemic stroke—Reply. *JAMA* 2014;312:961–962.
17. Smith-Bindman R, Miglioretti DL, Johnson E, et al. Use of diagnostic imaging studies and associated radiation exposure for patients enrolled in large integrated health care systems, 1996–2010. *JAMA* 2012;307:2400–2409. [PubMed: 22692172]
18. Miglioretti DL, Johnson E, Williams A, et al. The use of computed tomography in pediatrics and the associated radiation exposure and estimated cancer risk. *JAMA Pediatr* 2013;167:700–707. [PubMed: 23754213]
19. Blumich B, Singh K. Desktop NMR and its applications from materials science to organic chemistry. *Angew Chem Int Ed Engl* 2018;57:6996–7010. [PubMed: 29230908]
20. Danieli E, Mauler J, Perlo J, Blumich B, Casanova F. Mobile sensor for high resolution NMR spectroscopy and imaging. *J Magn Reson* 2009;198:80–87. [PubMed: 19217330]
21. Perlo J, Demas V, Casanova F, et al. High-resolution NMR spectroscopy with a portable single-sided sensor. *Science* 2005;308:1279. [PubMed: 15817815]
22. Perlo J, Silletta EV, Danieli E, et al. Desktop MRI as a promising tool for mapping intra-aneurismal flow. *Magn Reson Imaging* 2015;33:328–335. [PubMed: 25527392]

23. Danieli E, Perlo J, Blumich B, Casanova F. Highly stable and finely tuned magnetic fields generated by permanent magnet assemblies. *Phys Rev Lett* 2013;110:180801. [PubMed: 23683185]
24. Halbach K Design of permanent multipole magnets with oriented rare earth cobalt material. *J Nucl Instrum Methods* 1980;69:1–10.
25. Raich H, Blumler P. Design and construction of a dipolar Halbach array with a homogeneous field from identical bar magnets: NMR mandhalas. *Conc Magn Reson* 2004;23B:16–25.
26. Johns M, Fridjonsson EO, Voigh S, Haber A (eds.). *Mobile NMR and MRI, developments and applications*. Cambridge, UK: Royal Society of Chemistry; 2016.
27. Voda MA, van Duynhoven J. Benchtop-NMR-food: Solid fat content determination and emulsion droplet sizing. In: Johns M, Fridjonsson EO, Voigh S, Haber A, eds. *Mobile NMR and MRI, developments and applications*. Cambridge, UK: Royal Society of Chemistry; 2016. p 86–106.
28. Perlo J, Casanova F, Blumich B. Ex situ NMR in highly homogeneous fields: 1H spectroscopy. *Science* 2007;315:1110–1112. [PubMed: 17218492]
29. Blumich B, Blumler P, Eidmann G, et al. The NMR-mouse: Construction, excitation, and applications. *Magn Reson Imaging* 1998;16:479–484. [PubMed: 9803893]
30. Blumich B, Casanova F, Perlo J, Presciutti F, Anselmi C, Doherty B. Noninvasive testing of art and cultural heritage by mobile NMR. *Acc Chem Res* 2010;43:761–770. [PubMed: 20345119]
31. He Z, He W, Wu J, Xu Z. The novel design of a single-sided MRI probe for assessing burn depth. *Sensors* 2017;17(3).
32. Koruda MJ, Zimble A, Settle RG, et al. Assessing burn wound depth using in vitro nuclear magnetic resonance (NMR). *J Surg Res* 1986;40:475–481. [PubMed: 3736031]
33. Van Landeghem M, Danieli E, Perlo J, Blumich B, Casanova F. Low-gradient single-sided NMR sensor for one-shot profiling of human skin. *J Magn Reson* 2012;215:74–84. [PubMed: 22244451]
34. Backhouse L, Dias M, Gorce JP, Hadgraft J, McDonald PJ, Wiechers JW. GARField magnetic resonance profiling of the ingress of model skin-care product ingredients into human skin in vitro. *J Pharm Sci* 2004;93:2274–2283. [PubMed: 15295788]
35. McDonald PJ, Akhmerov A, Backhouse LJ, Pitts S. Magnetic resonance profiling of human skin in vivo using GARField magnets. *J Pharm Sci* 2005;94:1850–1860. [PubMed: 15986454]
36. Casanova F, Blumich B. Two-dimensional imaging with a single-sided NMR probe. *J Magn Reson* 2003;163:38–45. [PubMed: 12852905]
37. Perlo J, Casanova F, Blumich B. 3D imaging with a single-sided sensor: An open tomograph. *J Magn Reson* 2004;166:228–235. [PubMed: 14729034]
38. Hurlimann MD, Heaton NJ. NMR well logging. In: Johns M, Findjonson EO, Vogt S, Haber A, eds. *Mobile NMR and MRI; developments and applications*. Cambridge, UK: Royal Society of Chemistry; 2016. p 11–79.
39. McDaniel PC, Cooley CZ, Stockmann JP, Wald LL. The MR Cap: A single-sided MRI system designed for potential point-of-care limited field-of-view brain imaging. *Magn Reson Med* 2019 (in press).
40. Promaxo. MRI for live diagnosis and treatment in a physicians office 2019. Available from: <https://promaxo.com/>.
41. Rubin GD. Costing in radiology and health care: Rationale, relativity, rudiments, and realities. *Radiology* 2017;282:333–347. [PubMed: 28099106]
42. Managing high value capital equipment in the NHS in England. In: Health Do, ed. London: National Audit Office, Stationery Office; 2011.
43. Obyn C, Cleemput I. The capital cost and productivity of MRI in a Belgian setting. *JBR-BTR* 2010;93:92–96. [PubMed: 20524518]
44. Panel discussion. ISMRM Workshop on Accessible MRI; 2019. New Dehli, India.
45. Lvovsky Y, Stautner EW, Zhang T. Novel technologies and configurations of superconducting magnets for MRI. *Supercon Sci Technol* 2013; 26(093001).
46. Cosmus TC, Parizh M. Advances in whole-body MRI magnets. *IEEE Trans Appl Supercond* 2011;21:2104–2109.

47. Xu H, Conolly SM, Scott GC, Macovski A (eds.). Fundamental scaling relations for homogeneous magnets. In: Proc 7th Annual Meeting ISMRM, Philadelphia; 1999. p 475.
48. Parizh M, Lvovsky Y, Sumption M. Conductors for commercial MRI magnets beyond NbTi: Requirements and challenges. *Supercond Sci Technol* 2017;30:014007. [PubMed: 28626340]
49. Anderson ST. Economics, helium, and the U.S. Federal Helium Reserve: Summary and outlook. *Nat Resour Res* 2018;27:455–477.
50. Hirayama T, Morie T, Xu M. Experimental investigation of cooling capacity of 4K pulse tube cryocooler in magnetic fields. *IOP Conf Ser: Mater Sci Eng* 2018;502:012035.
51. Merhar SL, Tkach JA, Woods JC, et al. Neonatal imaging using an on-site small footprint MR scanner. *Pediatr Radiol* 2017;47:1001–1011. [PubMed: 28470389]
52. Panther A, Thevathasen G, Connell IRO, et al. A dedicated head-only MRI scanner for point-of-care imaging. In: Proc 27th Annual Meeting ISMRM, Montreal; 2019. p 3679.
53. Servick K, Cheap portable scanners could transform brain imaging. But how will scientists deliver the data? *Science* 2019 [Epub ahead of print].
54. Tenaud P, Lemaire H, Vial F. Recent improvements in NdFeB sintered magnets. *J Magn Magn Mater* 1991;101:328–332.
55. Miyamoto T, Sakurai H, Takabayashi H, Aoki M. A development of a permanent magnet assembly for MRI devices using Nd-Fe-B material. *IEEE Trans Magn* 1989;25:3907–3909.
56. Nakagomi M, Kajiwara M, Matsuzaki J, et al. Development of a small car-mounted magnetic resonance imaging system for human elbows using a 0.2T permanent magnet. *J Magn Reson* 2019;304:1–6. [PubMed: 31063952]
57. Blumler P, Casanova F. Hardware developments: Halbach magnet arrays. In: Johns M, Findjonson EO, Vogt S, Haber A, eds. *Mobile NMR and MRI; developments and applications*. Cambridge UK: Royal Society of Chemistry; 2016. p 133–155.
58. Cooley CZ, Haskell MW, Cauley SF, et al. Design of sparse Halbach magnet arrays for portable MRI using a genetic algorithm. *IEEE Trans Magn* 2018;54(1).
59. Cooley CZ, Stockmann JP, Armstrong BD, et al. Two-dimensional imaging in a lightweight portable MRI scanner without gradient coils. *Magn Reson Med* 2015;73:872–883. [PubMed: 24668520]
60. O'Reilly T, Wouter T, Winter L, Webb A (eds.). Design of a homogeneous large-bore Halbach array for low field MRI. In: Proc 27th Annual Meeting ISMRM, Montreal; 2019.
61. Blumler P Proposal for a permanent magnet system with a constant gradient mechanically adjustable in direction and strength. *Conc Magn Reson* 2016;46:41–8.
62. Vogel MW, Guridi RP, Su J, Vegh V, Reutens DC. 3D-spatial encoding with permanent magnets for ultra-low field magnetic resonance imaging. *Sci Rep* 2019;9:1522. [PubMed: 30728414]
63. Sarty GE. Cyclic generalized projection MRI. *Magn Reson Imaging* 2015;33:304–311. [PubMed: 25532468]
64. Ren ZH, Mu WC, Huang SY. Design and optimization of a ring-pair permanent magnet array for head imaging in a low-field portable MRI system. *IEEE Trans Magn* 2019;55:1–8.
65. Lother S, Schiff SJ, Neuberger T, Jakob PM, Fidler F. Design of a mobile, homogeneous, and efficient electromagnet with a large field of view for neonatal low-field MRI. *MAGMA* 2016;29:691–698. [PubMed: 26861046]
66. Obungoloch J, Harper JR, Consevage S, et al. Design of a sustainable prepolarizing magnetic resonance imaging system for infant hydrocephalus. *MAGMA* 2018;31:665–676. [PubMed: 29644479]
67. Kraus RH, Espy MA, Magnelind PE, Volegov PL. *Ultra-low field nuclear magnetic resonance, a new MRI regime*. Oxford, UK: Oxford University Press; 2014.
68. Macovski A, Conolly S. Novel approaches to low-cost MRI. *Magn Reson Med* 1993;30:221–230. [PubMed: 8366803]
69. Matter NI, Scott GC, Venook RD, et al. Three-dimensional prepolarized magnetic resonance imaging using rapid acquisition with relaxation enhancement. *Magn Reson Med* 2006;56:1085–1095. [PubMed: 17029228]

70. Lee SK, Mossle M, Myers W, et al. SQUID-detected MRI at 132 microT with T1-weighted contrast established at 10 microT–300 mT. *Magn Reson Med* 2005;53:9–14. [PubMed: 15690496]
71. Savukov IM, Zotev VS, Volegov PL, et al. MRI with an atomic magnetometer suitable for practical imaging applications. *J Magn Reson* 2009;199:188–191. [PubMed: 19435672]
72. Zotev VS, Matlashov AN, Volegov PL, et al. Microtesla MRI of the human brain combined with MEG. *J Magn Reson* 2008;194:115–120. [PubMed: 18619876]
73. Zotev VS, Owens T, Matlashov AN, Savukov IM, Gomez JJ, Espy MA. Microtesla MRI with dynamic nuclear polarization. *J Magn Reson* 2010;207:78–88. [PubMed: 20843715]
74. Tsai LL, Mair RW, Rosen MS, Patz S, Walsworth RL. An open-access, very-low-field MRI system for posture-dependent ³He human lung imaging. *J Magn Reson* 2008;193:274–285. [PubMed: 18550402]
75. Sarracanie M, LaPierre CD, Salameh N, Waddington DE, Witzel T, Rosen MS. Low-cost high-performance MRI. *Sci Rep* 2015;5:15177. [PubMed: 26469756]
76. Griswold MA, Jakob PM, Heidemann RM, et al. Generalized autocalibrating partially parallel acquisitions (GRAPPA). *Magn Reson Med* 2002;47:1202–1210. [PubMed: 12111967]
77. Pruessmann KP, Weiger M, Scheidegger MB, Boesiger P. SENSE: Sensitivity encoding for fast MRI. *Magn Reson Med* 1999;42:952–962. [PubMed: 10542355]
78. Duer-Jensen A, Vestergaard A, Dohn UM, et al. Detection of rheumatoid arthritis bone erosions by two different dedicated extremity MRI units and conventional radiography. *Ann Rheum Dis* 2008;67:998–1003. [PubMed: 17984195]
79. Gold G, Theodorou D, Blair T, et al. (eds.). MR imaging of the wrist with a portable extremity scanner. In: *Proc 7th Annual Meeting ISMRM, Philadelphia; 1999.* p 2039.
80. Crues JV, Shellock FG, Dardashti S, James TW, Troum OM. Identification of wrist and metacarpophalangeal joint erosions using a portable magnetic resonance imaging system compared to conventional radiographs. *J Rheumatol* 2004;31:676–685. [PubMed: 15088291]
81. Dietrich BE, Brunner DO, Wilm BJ, Barmet C, Pruessmann KP. Continuous magnetic field monitoring using rapid re-excitation of NMR probe sets. *IEEE Trans Med Imaging* 2016;35:1452–1462. [PubMed: 26742126]
82. Vannesjo SJ, Graedel NN, Kasper L, et al. Image reconstruction using a gradient impulse response model for trajectory prediction. *Magn Reson Med* 2016;76:45–58. [PubMed: 26211410]
83. Blucher C, Han H, Hoffmann W, et al. (eds.). COSI transmit: Open source soft-and hardware transmission system for traditional and rotating MR. In: *Proc 25th Annual Meeting ISMRM, Honolulu; 2017.* p 1055.
84. Gudino N, de Zwart JA, Duan Q, et al. Optically controlled on-coil amplifier with RF monitoring feedback. *Magn Reson Med* 2018;79:2833–2841. [PubMed: 28905426]
85. Gudino N, Duan Q, de Zwart JA, et al. Optically controlled switchmode current-source amplifiers for on-coil implementation in high-field parallel transmission. *Magn Reson Med* 2016;76:340–349. [PubMed: 26256671]
86. Twieg M, Griswold MA. High efficiency radiofrequency power amplifier module for parallel transmit arrays at 3 Tesla. *Magn Reson Med* 2017;78:1589–1598. [PubMed: 27797109]
87. Sporrer B Integrated broadband receivers for magnetic resonance imaging. Zurich, Switzerland: ETH Zurich; 2017.
88. Sporrer B, Wu L, Bettini L, et al. A fully integrated dual-channel on-coil CMOS receiver for array coils in 1.5-10.5 T MRI. *IEEE Trans Biomed Circuits Syst* 2017;11:1245–1255. [PubMed: 29293422]
89. Tang W, Wang W, Liu W, et al. A home-built digital optical MRI console using high-speed serial links. *Magn Reson Med* 2015;74:578–588. [PubMed: 25105249]
90. Stang PP, Conolly SM, Santos JM, Pauly JM, Scott GC. Medusa: A scalable MR console using USB. *IEEE Trans Med Imaging* 2012;31:370–379. [PubMed: 21954200]
91. Hasselwander CJ, Cao Z, Grissom WA. gr-MRI: A software package for magnetic resonance imaging using software defined radios. *J Magn Reson* 2016;270:47–55. [PubMed: 27394165]
92. Anand S, Stockmann JP, Wald LL, Witzel T (eds.). A low-cost (<\$500 USD) FPGA-based console capable of real-time control. In: *Proc 26th Annual Meeting ISMRM, Paris; 2018.* p 948.

93. Ocra open MRI Available from: <https://openmri.github.io/ocra/>.
94. Winter LB. Open source magnetic resonance imaging: From the community to the community 2019. Available from: opensourceimaging.org.
95. Fessler J Model-based image reconstruction for MRI. IEE Signal Proc Mag 2010;27:81–89.

Author Manuscript

Author Manuscript

Author Manuscript

Author Manuscript



FIGURE 1: Marie Curie circa 1915 shown with one of her mobile x-ray units used during WWI. Source: http://www.nobelprize.org/nobel_prizes/physics/articles/curie/images/c_truck.jpg.

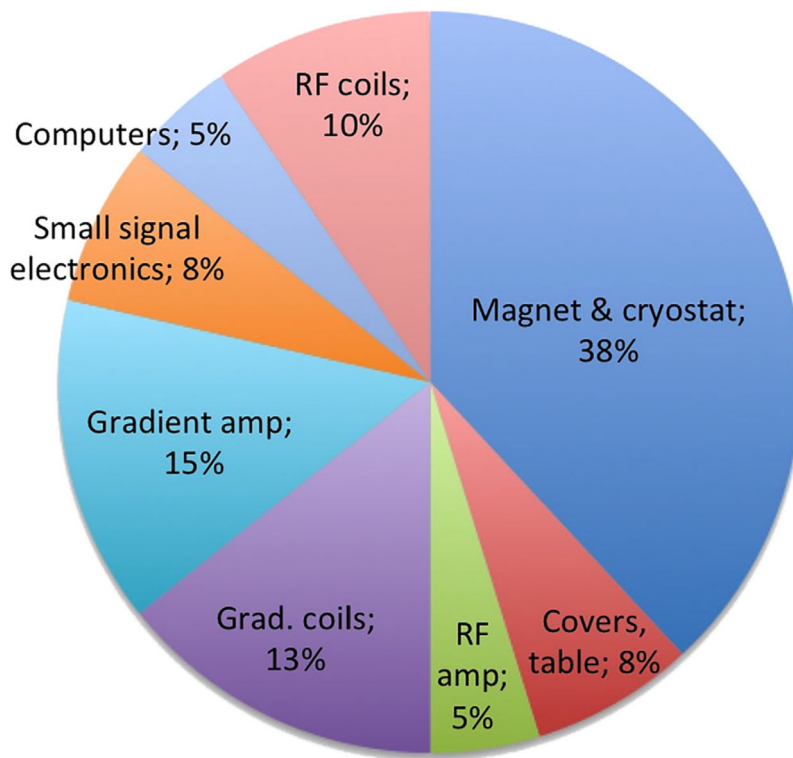


FIGURE 2: Estimate of the relative component costs within a low-end conventional 1.5T scanner. Costs are estimated for high-volume commodity production (runs of ~1000 per year) and would be considerably higher for one-off, or laboratory instrumentation. Note that a low-end system with a market price of about \$800,000 USD and a 4× markup over components cost suggests a total components cost of \$200,000 USD leaving a cost of about \$75,000 USD for the magnet and cryostat. Costs, of course, depend on the detailed specifications, and are treated as proprietary figures in the industry. Thus, these estimates are based on the authors’ intuition and not specific data.

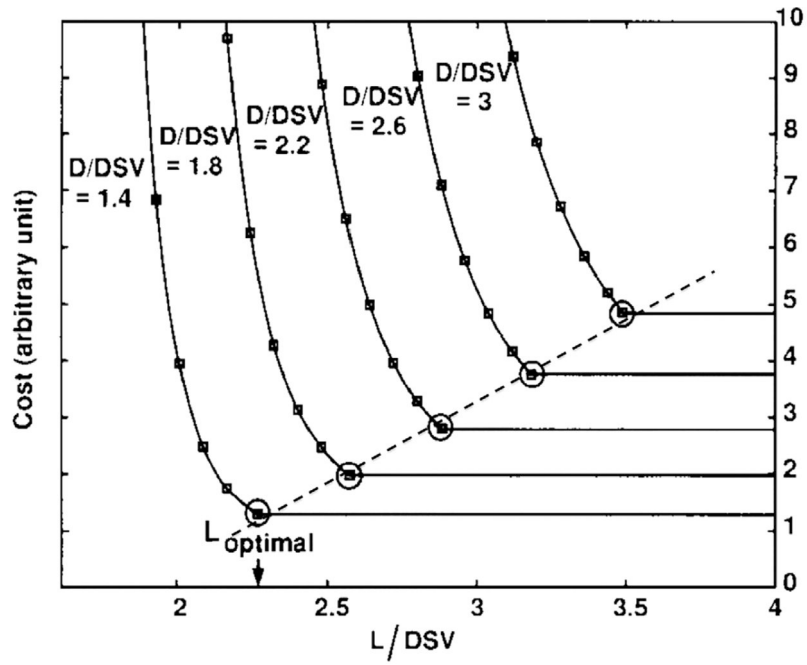


FIGURE 3:

Magnet wire cost as a function of magnet length L and bore diameter D (both expressed as a fraction of the diameter of the homogeneous region, DSV) for superconducting solenoid designs. This design analysis shows the rapid rise in cost for short magnets and constructing a homogeneous magnet shorter than L_{opt} quickly becomes expensive (a 1 ppm homogeneity in the DSV was used in this analysis). For all the designs studied, the optimal length followed the relationship $L_{opt} = 1.18 \text{ DSV} + 0.77 \text{ D}$. From Xu et al. In: Proc 7th Annual Meeting ISMRM, Philadelphia; 1999. p 475.⁴⁷

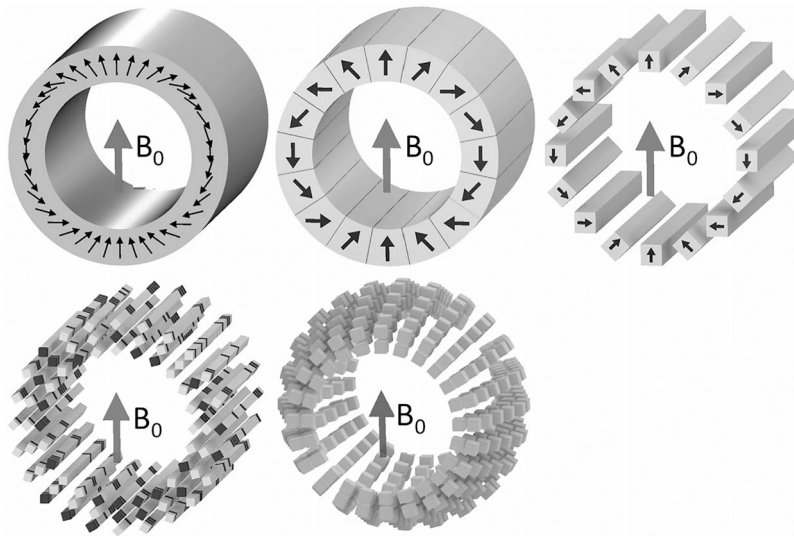


FIGURE 4:

Halbach cylinder designs of potential interest for low-field MRI. In the Halbach cylinder, a nearly uniform transverse field is produced inside the cylinder if the magnetic moment of the magnetized material is phased from 0 to 4π azimuthally. Note that this is similar to the phase relationship for a birdcage coil where a 0 to 2π azimuthal phase relationship is used. Top row shows an ideal cylinder with continuous magnetization and a more practical approximation comprising keystone-shaped sections. Far top right shows a simpler to construct configuration using only identical rectangular blocks and with all the magnetization vectors normal to a face. The phase relationship comes only from rotations of the blocks. The bottom row shows further optimizations allowing degrees of freedom to be adjusted to achieve a target field pattern (typically either a uniform field or a monotonic gradient) despite the imperfections of the array (eg, finite cylinder and sparse population). One option is to maintain linear rungs of material but vary the material. A second approach is to maintain rings of material but allow varying diameters.

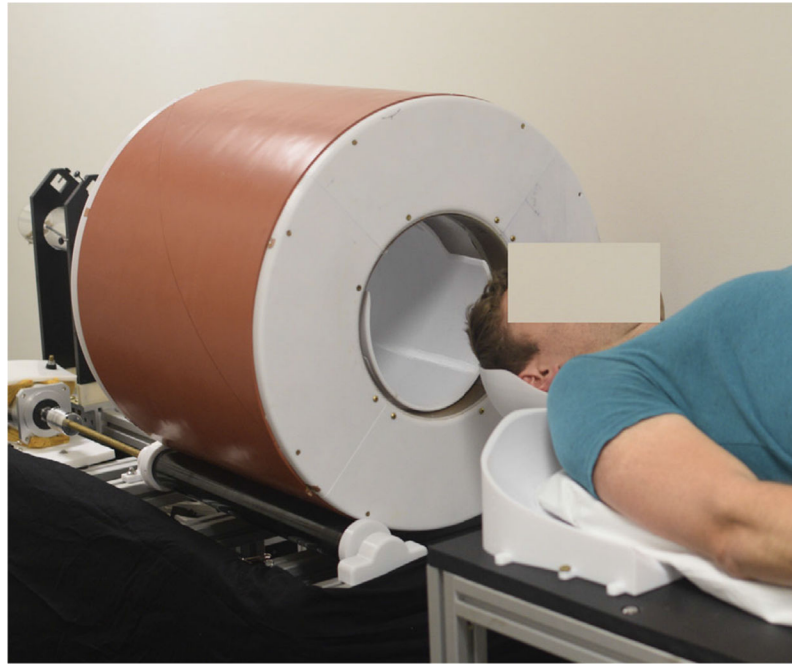


FIGURE 5:

A prototype portable brain MRI scanner based on the Halbach permanent magnet described in Cooley et al (IEEE Trans Magn 2018;54)⁵⁸ and configured for rotational encoding as in Cooley et al (Magn Reson Med 2015;73:872–883).⁵⁹ The magnet weighs ~125 kg and achieves an 80 mT B_0 field.